processes

MDPI

Article

Supercritical Water Oxidation of Nuclear Cation Exchange Resins: Process Optimization and Reaction Mechanism

Tiantian Xu [1,*], Yanhui Li [2,*], Shuzhong Wang [2], Donghai Xu [2], Qian Zhang [1], Yabin Jin [1] and Wenhan Song [1]

[1] School of Energy and Architecture, Xihang University, Xi'an 710077, China
[2] Key Laboratory of Thermo-Fluid Science and Engineering of MOE, School of Energy and Power Engineering, Xi'an Jiaotong University, Xi'an 710049, China
* Correspondence: tiantianxu@xaau.edu.cn (T.X.); yhli19@sina.com (Y.L.)

Abstract

This study conducted a systematic investigation of the degradation pathway and process optimization of strong acid cation exchange resins subjected to SCWO. Controlled experiments evaluated the effects of operating temperature, oxidant stoichiometry, initial organic concentration, and residence time. RSM was utilized to refine the operating parameters, and a second-order regression model (R^2 = 0.9951) was established to predict COD removal (R_{COD}), valid within experimental ranges: reaction temperature 400–500 °C, oxidant stoichiometry 80–150%, initial COD 10,000–100,000 mg·L^{-1}, and residence time 1–10 min. COD-dependent NaOH addition could enhance degradation efficiency. The R_{COD} was sensitive to operating temperature, oxidant stoichiometry, and residence time. Under the optimized conditions of 472 °C, oxidant stoichiometry of 137%, initial COD of 77,216 mg·L^{-1}, and residence time of 4.9 min with the addition of 1.74 wt% NaOH, the R_{COD} reached 99.92%, which was in close agreement with model predictions. GC-MS analysis of intermediates revealed that sulfonic groups dissociated early, followed by aromatic compounds, particularly phenol, undergoing ring-opening and oxidation to small carboxylic acids and aliphatic species, which were ultimately mineralized to CO_2 and H_2O. These findings provide mechanistic insight into resin decomposition and offer a scientific basis for the safe treatment of radioactive waste resins using SCWO.

Keywords: supercritical water oxidation; cation exchange resin; radioactive waste; response surface methodology; process optimization; reaction intermediates; degradation pathway

check for updates

Academic Editors: Leandro Ferreira Pinto and Lúcio Cardozo Filho

Received: 31 August 2025
Revised: 5 October 2025
Accepted: 11 October 2025
Published: 13 October 2025

Citation: Xu, T.; Li, Y.; Wang, S.; Xu, D.; Zhang, Q.; Jin, Y.; Song, W. Supercritical Water Oxidation of Nuclear Cation Exchange Resins: Process Optimization and Reaction Mechanism. *Processes* **2025**, *13*, 3249. https://doi.org/10.3390/pr13103249

Copyright: © 2025 by the authors. Licensee MDPI, Basel, Switzerland. This article is an open access article distributed under the terms and conditions of the Creative Commons Attribution (CC BY) license (https://creativecommons.org/licenses/by/4.0/).

1. Introduction

Radioactive spent ion-exchange resin, identified by the International Atomic Energy Agency as a "problematic" waste stream, exhibits dispersibility, radiolytic instability, water absorption, swelling, and corrosiveness [1]. With the continued operation of nuclear power plants and the commissioning of new reactors, its generation is steadily increasing, yet no industrially viable treatment technology exists. Disposal remains subject to stringent, long-term regulation extending over centuries. As temporary storage facilities approach capacity, efficient strategies for resin minimization and mineralization have become an urgent necessity. Efficient treatment of spent exchange resins is crucial for mitigating the environmental impact of radioactive waste. It also holds broader significance for nuclear facility decommissioning and long-term waste management. Achieving high mineralization rates ensures more thorough decomposition of organic components, thereby supporting the development of sustainable radioactive waste disposal strategies.

As a promising environmentally friendly technology for radioactive waste treatment, supercritical water oxidation (SCWO) has received significant interest in recent decades owing to its excellent capability for decomposing refractory organic wastes. SCWO exploits the unique properties of water in the supercritical state, including lower density, a minimal ionization constant, lower dielectric constant, and weakened hydrogen bonding. This technology offers notable advantages for radioactive organic waste management: reactions occur within seconds to minutes [2,3], organic compounds are almost completely degraded, and operating at moderate temperatures helps minimize radionuclide release into exhaust streams [4]. The extremely low solubility of inorganic salts in supercritical water facilitates efficient nuclide separation, and highly aqueous wastes can be treated directly without drying pretreatment [5,6].

Ion exchange resins are utilized to eliminate corrosion products, fission products, and other contaminants from the water circulation system, thereby ensuring water quality and supporting the efficient operation of nuclear reactors. These resins are styrene-divinylbenzene copolymers, and those functionalized with strongly acidic or basic groups are widely used for their pH-independent performance. Acidic cationic resins contain $–SO_3H$ groups, whereas basic anionic resins incorporate $–N(CH_3)_3OH$ groups. In terms of composition, cation exchange resins typically contain ~16 wt% sulfur (dry basis), whereas anion exchange resins contain ~3.2–4.2 wt% nitrogen (dry basis). Both types usually have a water content of approximately 55–60 wt% [7,8].

Previous studies have demonstrated that SCWO can achieve satisfactory treatment efficiencies for nuclear waste resins. Sugiyama et al. [9] reported that radioactive anion exchange resins achieved removal efficiencies of 86% at 400 °C and 96% at 450 °C under 43 MPa for up to 60 min using RuO_2 as a catalyst, with trace amounts of oily by-products detected. Leybros et al. [10] reported that anion resins could reach 99.95% degradation under an oxidant stoichiometry of 150–170%. Kim et al. [7] reported that cation exchange resins achieved 99.68% degradation under SCWO at 358 °C, with a COD of 25,000 mg/L, an oxidant stoichiometry of 160%, 0.615 wt% of NaOH, for 22.5 min. In contrast, anion exchange resins with a COD of 50,000 mg/L reached over 99% removal at 520 °C with a residence time of 1.25 min [11]. Existing studies have primarily examined the influence of single parameters on cationic resin degradation, while multi-parameter optimization has been more extensively investigated for anionic resins [12]. In general, higher temperature, increased oxidant dosage, and extended reaction time improve the removal efficiency of organics in SCWO [13]. However, excessively severe operating parameters may accelerate material corrosion, increase capital costs, and lead to higher energy consumption [14]. Thus, optimizing the key reaction parameters is essential to achieve both high efficiency and operational feasibility.

To date, limited research has addressed the systematic optimization of cationic resin degradation under SCWO, despite evidence that strongly basic anion resins exhibit greater resistance than cation resins at low concentrations due to persistent quaternary ammonium degradation products [10,11]. Moreover, the role of additives such as NaOH in modifying reaction environments and influencing degradation pathways of cation resins has not been thoroughly elucidated, leaving important mechanistic questions unresolved.

As outlined above, this work systematically investigated the SCWO of cation exchange resins. First, the study evaluated the degradation efficiency under a range of initial concentrations with NaOH addition. Second, Response Surface Methodology (RSM) was employed to optimize the key operating parameters—temperature, oxidant stoichiometry, initial COD concentration, and residence time, thereby revealing their complex interactions. Finally, and most importantly, it elucidates the degradation pathway by tracking the transformation of representative intermediates, providing crucial insight into the underlying

reaction mechanisms. Together with our prior work on anion resins [12], this research provides valuable experimental data and establishes an optimized operational framework for the safe and efficient disposal of radioactive ion-exchange resins. It also lays a foundation for further development of SCWO technology in nuclear waste management strategies.

2. Experiments

2.1. Materials and Analytical Methods

Fresh cation exchange resins were used to ensure consistent and reproducible conditions. Actual radioactive spent resins can undergo radiation-induced structural changes, which could affect their degradation in SCWO. This approach also facilitates future studies on irradiated resins. In this study, a fresh strong acid cation exchange resin (ZGA NR50), supplied by Zhejiang Zhengguang Industry Co., Ltd. (Ningbo, China), was used to simulate radioactive waste resin. This resin is a copolymer of styrene cross-linked with divinylbenzene and functionalized with sulfonic acid (–SO_3H) groups. It is a typical matrix for this type of strong acid cation exchangers. Fresh resin particles were milled into a fine powder, vacuum-dried for three days, and subsequently sieved to obtain particles smaller than 90 μm. The elemental composition of the cationic resin is summarized in Table 1. COD concentrations in the resin samples and in the post-reaction liquid were measured using a NOVA 60 spectrophotometer (Merck KGaA, Darmstadt, Germany). The resin's initial COD was 1461.73 $mg \cdot g^{-1}$ on a dry weight basis.

Table 1. Elemental composition of the cationic resin on a dry weight basis.

Mass Fraction of Sample (%)	C	H	O	S
Cationic resin	41.79	5.89	36.67	15.65

Analysis of the major liquid-phase intermediates was carried out by GC/MS–QP2010 Ultra (Shimadzu Corporation, Kyoto, Japan). For separation, the GC–MS employed an Rxi-5Sil MS column (Restek Corporation, Thomasville, PA, USA) measuring 30 m in length with 0.25 mm I.D. and 0.25 μm film thickness. For each run, 1 μL of the sample was injected with a 2:1 split ratio, and helium served as the carrier gas at 3 mL/min. The oven temperature was programmed in three stages, increasing from 50 °C (held for 2 min) to 80 °C at 4 °C/min (held for 2 min), then to 160 °C at 5 °C/min (held for 3 min), and finally to 280 °C at 4.5 °C/min, where it was maintained for 10 min. Electron impact (EI) mass spectra were recorded over a 15–400 m/z range.

2.2. Apparatus and Experimental Methods

All experiments were conducted on a laboratory-scale SCWO system. To achieve rapid heating and cooling as well as precise reaction timing, intermittent reactors were operated together with a Techne SBL-2D fluidized sand bath (Figure 1). The 9.4 mL reactors employ 316 stainless steel tubing with bite fittings. Temperatures as high as 580 °C and pressures up to 34 MPa can be achieved in the reactors. Real-time temperature measurements are obtained via a thermocouple positioned in the center of the reactor. The reactor was charged with a measured amount of resin, deionized water, and hydrogen peroxide. Prior to the reaction, the reaction vessel was purged with helium for 5 min, and the connections were then tightened to ensure a sealed system. The dosages of resin, deionized water, and hydrogen peroxide were determined according to vessel volume, operating temperature, and system pressure, and were further validated in preliminary experiments. NaOH was added based on the initial COD concentration and prepared as a corresponding solution in deionized water [12]. The reactor was submerged in a preheated fluidized sand bath, and the temperature was monitored and maintained within ±2 °C. After the reaction vessel

attained the target operating temperature, a stopwatch was used to track the reaction time. At the end of the set reaction time, the reactor was rapidly cooled in room-temperature water to below the supercritical temperature to stop the reaction. It was then maintained for at least 5 h to reach gas–liquid equilibrium before analysis. The resulting liquid was collected for subsequent analysis. Detailed descriptions of the experimental setup and procedure have been provided in our previous publications [12].

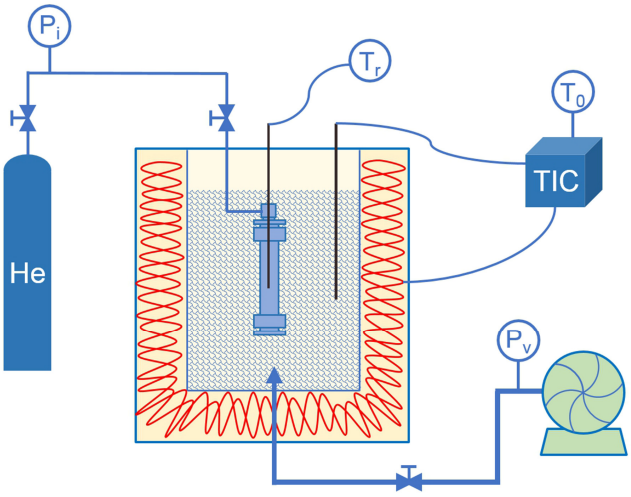


Figure 1. Experimental apparatus.

2.3. Calculation Procedures

The R_{COD}, representing the chemical oxygen demand removal rate, was used to evaluate organic matter degradation in the SCWO process, and the response parameter for R_{COD} is defined below:

$$R_{COD}(\%) = \frac{[COD]_i - [COD]_r}{[COD]_i} \times 100 \quad (1)$$

Here, $[COD]_i$ and $[COD]_r$ represent the COD concentrations measured in the system before and after the SCWO reaction.

$[O_2]_{sto}$ represents the stoichiometric amount of oxidant and is defined as follows:

$$[O_2]_{sto}(\%) = \frac{[O_2]_i}{[COD]_i} \times 100 \quad (2)$$

$[O_2]_i$ corresponds to the oxidant concentration at the start of the reaction.

2.4. Design of Experiments

The experimental design applied the Central Composite Design (CCD) approach based on RSM to find the optimal process conditions for achieving the maximum R_{COD}. Using a five-level central composite design with four factors, the study evaluated the effects of operating temperature, oxidant stoichiometry, initial organic concentration, and residence time on the process. Each independent factor was assigned five coded levels ($-\alpha$, 1, 0, +1, $+\alpha$), where α = 1.682 for the four-factor CCD-RSM design. Table 2 provides both the experimental ranges and the associated coded and actual values.

Table 2. Actual process variable values for coded levels in SCWO cation resin experiments.

Operating Parameters	Unit	Code	Actual Values Corresponding to Coded Levels				
			−1.682	**−1**	**0**	**1**	**1.682**
Temperature	°C	*A*	400	420	450	480	500
Oxidant stoichiometry	%	*B*	80	94	115	136	150
Initial organic concentration	$mg \cdot L^{-1}$	*C*	10,000	28,243	55,000	81,757	100,000
Residence time	min	*D*	1.0	2.8	5.5	8.2	10.0

Based on the CCD experiments, a second-order quadratic model was established to represent the response, with inter-variable relationships expressed by the following equation [15]:

$$Y = \beta_0 + \sum_{i=1}^{k} \beta_i X_i + \sum_{i=1}^{k-1} \sum_{j=i+1}^{k} \beta_{ij} X_i X_j + \sum_{i=1}^{k} \beta_{ii} X_{ii}^2 \quad (3)$$

Equation (3) presents the response variable Y, with coefficients β_0, β_i, β_{ij}, and β_{ii} representing the intercept, linear, interaction, and quadratic terms, respectively. X_i and X_j denote the coded values for the five independent variables. Analysis of variance (ANOVA) was used to systematically evaluate the results.

To evaluate the association between the independent factors and the response, the complete set of experimental data was coded to develop a second-order polynomial model. In general, significant model terms are indicated when Prob > *F* is less than 0.0500, whereas values greater than 0.1000 usually suggest non-significance. The model can be refined by removing insignificant terms, except those required to maintain model hierarchy, when Prob > *F* exceeds 0.0500. A non-significant lack of fit indicates that the model adequately represents the experimental data, implying a low level of discrepancy between model predictions and measurements. Model adequacy is further indicated by the adequacy precision (AP) when the signal-to-noise ratio meets or exceeds 4. An appropriate model is indicated by an R^2 value above 0.8, calculated as the squared correlation coefficient. Moreover, a reliable model requires that the gap between Predicted R^2 and Adjusted R^2 remains within 0.2.

3. Discussion of Results

3.1. Effect of NaOH on Cation Resin Decomposition

Sulfonic functional groups in the cation-exchange resin generate sulfuric acid during SCWO, leading to a highly acidic reaction system [7,16]. During the SCWO process, organic compounds break down into acidic intermediates, which are subsequently oxidized into low-molecular-weight compounds. Excessive acidity in the system can inhibit the formation of acidic substances, thereby impeding the reaction and reducing the removal rate of organic matter. Acidic supercritical water oxidizing environments can also exacerbate material corrosion [17]. Therefore, the degradation of the cationic resin needs to be moderated by acid neutralization.

The impact of different NaOH dosages on cationic resin decomposition during SCWO is presented in Figure 2. The experiment was conducted under the following conditions: initial organic content corresponding to COD of 60,000 $mg \cdot L^{-1}$, pressure of 25 MPa, temperature of 460 °C, oxidant stoichiometry of 130%, and residence time of 5 min. The data illustrated that R_{COD} increased as the amount of NaOH added increased. Specifically, when 1.4 wt% was added at an initial COD concentration of 60,000 $mg \cdot L^{-1}$, the R_{COD} reached 98.47%. However, further increases in NaOH dosage did not significantly change the R_{COD}.

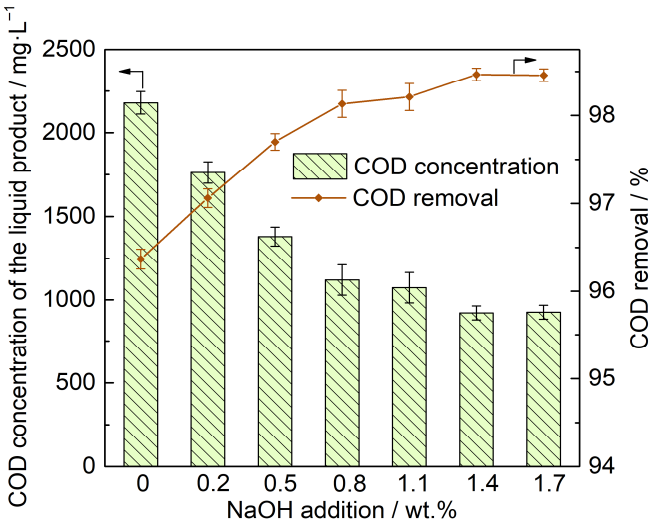


Figure 2. Effect of different NaOH additions on the degradation of cationic resin.

The concentration of sulfonic acid groups in the reaction system depends on the initial COD concentration, resulting in different amounts of NaOH required for neutralization. Therefore, the effect of the corresponding amount of added NaOH on the degradation of the cationic resin was investigated based on the sulfur content at different initial COD concentrations, as shown in Figure 3. Under NaOH addition, the R_{COD} of cation resin at different concentrations also increased significantly. Kim et al. [7] also reported that adding NaOH improves the degradation efficiency of cation resins. Lee et al. [18] found that NaOH inhibited the production of dimer intermediates during SCWO of phenol and o-chlorophenol, thereby promoting the degradation of organic matter. Hence, the addition of NaOH not only neutralizes the acid in the reaction process but also improves the degradation efficiency of organic matter.

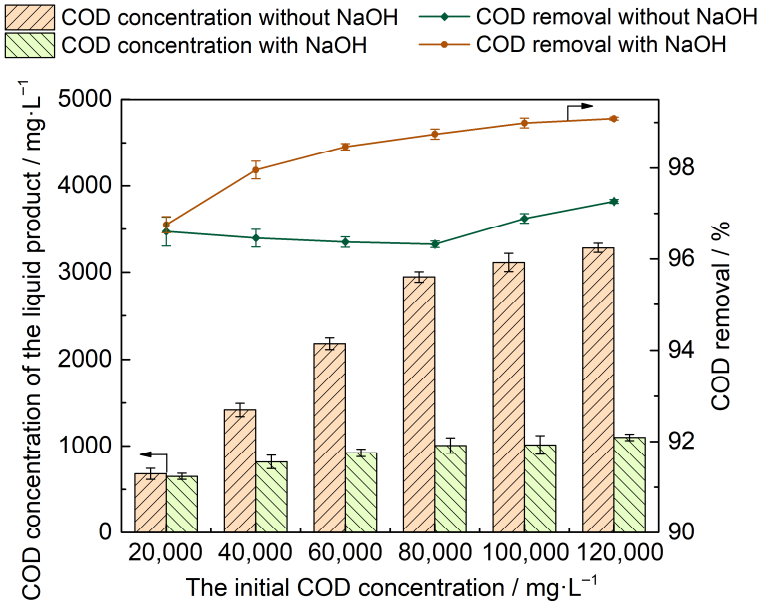


Figure 3. Effect of NaOH on cation resin degradation with different initial COD concentrations.

3.2. Decomposition of Cation Resin in SCWO

Table 3 illustrates the results of SCWO degradation of cation resin under designed experimental conditions and the predicted results based on the established model. The results showed significant differences in the efficiency of organic degradation in the SCWO

system under varying reaction conditions, with the R_{COD} ranging from 79.12% to 99.92%. It should be noted that the amount of NaOH added to the system varied with the COD concentration, as shown in the previous subsection. Specifically, for COD concentrations of 10,000 mg·L^{-1}, 28,243 mg·L^{-1}, 55,000 mg·L^{-1}, 81,757 mg·L^{-1}, and 100,000 mg·L^{-1}, the corresponding amounts of NaOH added were 0.26 wt%, 0.71 wt%, 1.30 wt%, 1.83 wt%, and 2.16 wt%, respectively.

Table 3. Experimental settings and measured results.

Parameters				Responses	
				Experimental	Predicted
A (°C)	*B* (%)	*C* (mg·L^{-1})	*D* (min)	R_{COD} (%)	R_{COD} (%)
420	136	81,757	8.2	94.78	94.79
450	80	55,000	5.5	88.72	88.97
450	150	55,000	5.5	98.64	98.89
400	115	55,000	5.5	79.12	79.37
450	115	100,000	5.5	95.32	95.63
480	94	81,757	8.2	92.06	91.38
450	115	10,000	5.5	92.67	92.85
450	115	55,000	5.5	96.01	96.10
420	136	28,243	8.2	92.45	92.09
450	115	55,000	10.0	97.08	97.33
450	115	55,000	1.0	91.13	91.38
450	115	55,000	5.5	95.46	96.10
480	136	28,243	2.8	96.74	96.81
450	115	55,000	5.5	96.58	96.10
480	136	81,757	2.8	99.92	99.51
450	115	55,000	5.5	96.26	96.10
500	115	55,000	5.5	98.56	98.81
420	94	81,757	2.8	83.67	83.94

3.3. Fitted Regression Model for Cation Resin in the SCWO Process

The accuracy and applicability of the updated R_{COD} model were evaluated via ANOVA, as shown in Table 4.

Table 4. Statistical parameters obtained from the ANOVA for the established model.

Source	Sum of Squares	df	Mean Square	*F*-Value	*p*-Value Prob > *F*
Model	590.24	12	49.19	134.54	<0.0001
A-Temperature	188.96	1	188.96	516.84	<0.0001
B-Oxidant stoichiometry	49.20	1	49.20	134.58	<0.0001
C-Initial organic concentration	9.36	1	9.36	25.60	0.0010
D-Residence time	17.70	1	17.70	48.42	0.0001
AB	3.92	1	3.92	10.72	0.0113
AD	5.36	1	5.36	14.67	0.0050
BC	2.17	1	2.17	5.95	0.0407
BD	24.89	1	24.89	68.09	<0.0001
A^2	91.81	1	91.81	251.13	<0.0001
B^2	8.80	1	8.80	24.08	0.0012
C^2	6.43	1	6.43	17.60	0.0030
D^2	5.69	1	5.69	15.57	0.0043
Residual	2.92	8	0.37		
Lack of fit	1.89	4	0.47	1.83	0.2863
Pure Error	1.03	4	0.26		
R^2 = 0.9951, AP = 42.333, Adj R^2 = 0.9877, Pred R^2 = 0.8712					

The R_{COD} model exhibited an *F*-value of 134.54 and a highly significant *p*-value (<0.0001), demonstrating excellent agreement with the experimental data. The model's Adequate Precision (AP) was 42.333, well above the threshold of 4. The R^2 value greater than 0.8 indicated that the established R_{COD} model could fit at least 99.51% of the experimental data. The Pred R^2 and Adj R^2 values were 0.8712 and 0.9877, respectively, with a reasonable difference of less than 0.2. Model diagnostic plots were used to assess the adequacy of the R_{COD} model. Figure 4a shows the normal probability plot of the residuals, where the points approximately lie along a straight line [19], indicating that the residuals were normally distributed and the model was appropriate for the experimental data. Figure 4b presented the residuals versus predicted values plot, in which the residuals were evenly and randomly distributed within a relatively narrow range from −3 to 3 [20], indicating a high fitting accuracy of the model. Figure 4c presented the comparison between the experimental and predicted values. Based on the information presented above, it could be concluded that the R_{COD} regression model obtained for characterizing cationic resin degradation in the process of SCWO was satisfactory and reliable. Insignificant terms such as *AC* and *CD* have been eliminated to improve the R_{COD} model. Equation (4) shows the modified regression model for R_{COD}. The model is valid within the specific experimental ranges investigated: reaction temperature 400–500 °C, oxidant stoichiometry 80–150%, initial COD concentration 10,000–100,000 mg·L^{-1}, and residence time 1–10 min.

$$R_{COD} = 96.10 + 5.78 \times A + 2.95 \times B + 0.83 \times C + 1.77 \times D + 1.09 \times AB - 1.27 \times AD + 0.52 \times BC + 2.74 \times BD - 2.48 \times A^2 - 0.77 \times B^2 - 0.66 \times C^2 - 0.62 \times D^2 \quad (4)$$

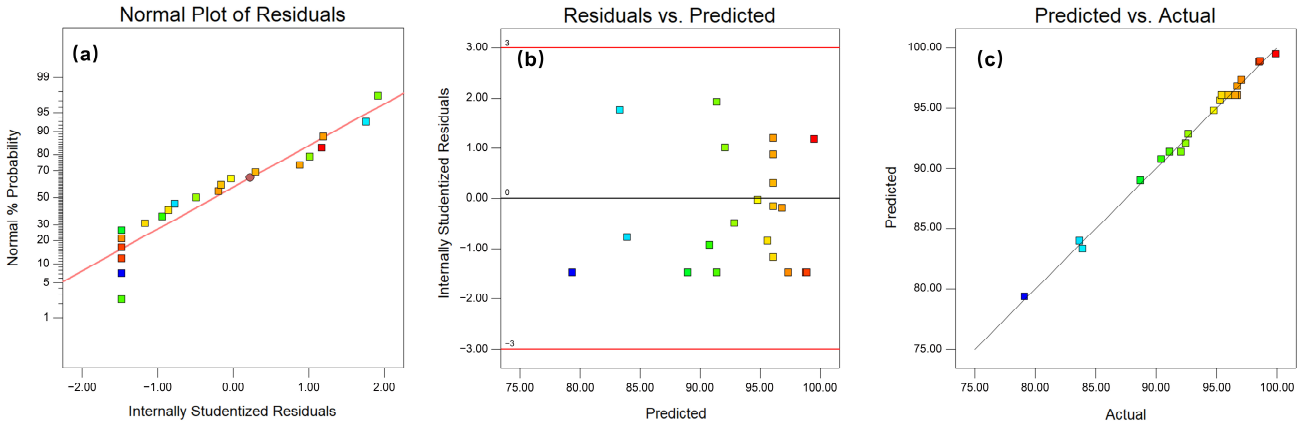


Figure 4. RSM diagnostic plots for (**a**) Normal plot of the residuals; (**b**) Residual vs. predicted; (**c**) Predicted vs. actual.

Figure 5 displays the 3D response surfaces and contour plots of R_{COD}, highlighting the interactions between the two most influential factor pairs in the model. A steeper surface indicates a stronger influence of the corresponding parameter on the response. The interaction between temperature and oxidant stoichiometry on resin R_{COD} is shown in Figure 5a. The plot shows that R_{COD} increased with both reaction temperature and oxidant stoichiometry, with temperature having a stronger effect than oxidant stoichiometry. Generally, higher temperature increases the number of activated reactant molecules in supercritical water. This promotes the degradation of organic compounds [21]. A moderate oxidant stoichiometry accelerates the reaction and enhances removal, whereas excessive levels reach a maximum without further improvement. Excess oxidant can generate a high concentration of OH•, which consumes H_2O_2 and produces the less reactive HO_2• (H_2O_2 + OH• → H_2O + HO_2•). This competitive pathway reduces oxidative effectiveness [8]. The

interaction of residence time and temperature is shown in Figure 5b. Temperature still exerts a greater effect on R_{COD} than reaction time. In SCWO, the reaction rate increases with residence time, allowing most organics to be gradually removed as reactant concentrations decline. However, beyond an optimal residence time, termination reactions dominate, weakening the positive effect of longer residence on contaminant removal [22,23]. Figure 5c shows the combined effect of oxidant stoichiometry and reaction time. The plot shows that the influence of oxidant stoichiometry was slightly greater than that of reaction time. This finding agrees with the ANOVA results (Table 4). The parameter influence on R_{COD} ranks as follows: temperature > oxidant stoichiometry > reaction time. A minor positive effect of the initial organic concentration on RCOD was also observed (Prob > F = 0.0010).

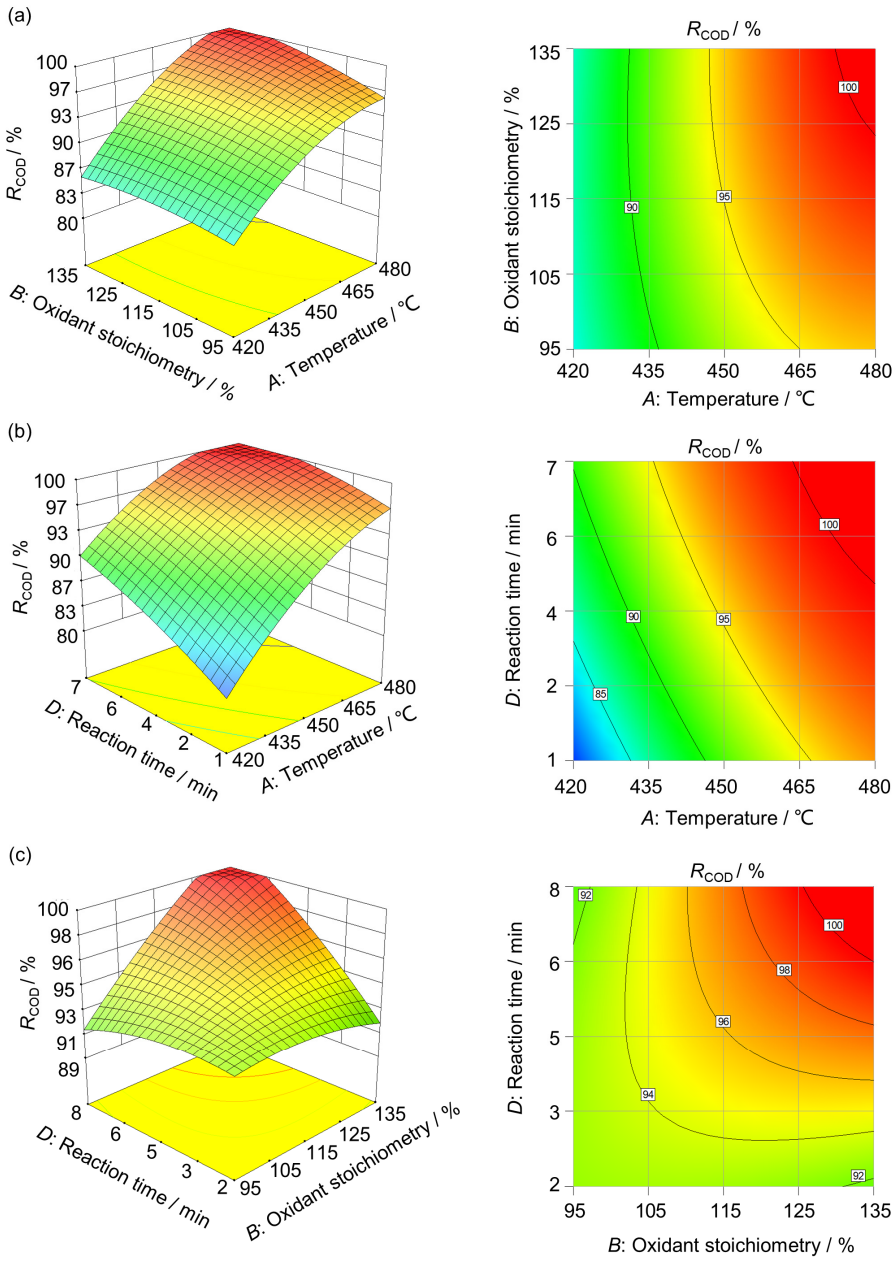


Figure 5. Three-dimensional R_{COD} response surfaces showing interactions between different factors: (**a**) operating temperature vs. oxidant stoichiometry (initial COD of 60,000 mg·L^{-1}, 4 min); (**b**) temperature vs. reaction time (initial COD of 60,000 mg·L^{-1}, oxidant stoichiometry 120%); (**c**) oxidant stoichiometry vs. reaction time (initial COD of 60,000 mg·L^{-1}, 450 °C).

3.4. Process Conditions Optimization

RSM is primarily employed to determine the system's optimal operating conditions or to locate regions that satisfy operational criteria [24]. For the R_{COD} response, all process variables were constrained within defined ranges [25,26]. R_{COD} reached its maximum in cationic resin SCWO under the most favorable conditions. Considering the degrading efficiency, the reaction was conducted at temperatures ranging from 450 to 490 °C. The oxidant stoichiometry range was chosen to be between 110% and 150%, balancing both degradation efficiency and system economy. The initial COD concentration ranged from 50,000–80,000 mg·L^{-1} to ensure practical use. Due to the practical size of the reactor, the reaction time was limited to 1–5 min.

The desirability function typically identifies multiple combinations of variable levels for which all responses are acceptable [25,27]. The desirability method applied in the response optimization procedure yielded multiple solutions, each corresponding to a set of reaction parameters. Two supplementary experiments were performed under the optimized conditions to verify the agreement between predicted and observed values, with initial COD concentrations of 77,216 mg·L^{-1} and 62,116 mg·L^{-1} and corresponding NaOH additions of 1.74 wt% and 1.45 wt%, respectively. As shown in Table 5, the experimental R_{COD} results closely matched the predictions, further validating the accuracy and reliability of the developed model for cationic resin SCWO. While the laboratory-scale experiments demonstrated clear trends in resin degradation and process optimization, further investigations on a pilot-scale SCWO system would be necessary to confirm scalability and evaluate practical applicability. This is particularly important for industrial implementation in the treatment of radioactive waste resins.

Table 5. Experimental verification under optimal conditions.

	Parameters				Responses	
					Predicted	Experimental
Number	***A* (°C)**	***B* (%)**	***C* (mg·L^{-1})**	***D* (min)**	R_{COD} [a] (%)	R_{COD} (%)
1	472	137	77,216	4.9	100	99.92
2	480	130	62,116	4.0	100	99.91

[a] R_{COD} predictions were approximated to the nearest 100%.

4. Mechanism of Degradation

4.1. Species Identification

GC–MS analysis of intermediates in the liquid phase after SCWO was used to propose the reaction pathway. At 25 MPa, 460 °C, and an initial COD of 60,000 mg·L^{-1}, three experiments were carried out with the addition of 1.4wt% NaOH. The residence times were 10 s, 1.0 min, and 3.7 min. Tables 6 and 7 list the intermediates detected in the effluent of each experiment.

Table 6. Primary intermediates in the liquid phase under 25 MPa and 460 °C with an initial COD of 60,000 mg·L^{-1} and a residence time of 10 s.

Compound	Formula	Peak Area Ratio/%
Ethylbenzene	C_8H_{10}	2.08
o-Xylene	C_8H_{10}	2.13
Benzaldehyde	C_7H_6O	8.93
Phenol	C_6H_6O	12.72
o-Cymene	$C_{10}H_{14}$	4.14
2-Methylphenol	C_7H_8O	3.12

Table 6. *Cont.*

Compound	Formula	Peak Area Ratio/%
Acetophenone	C_8H_8O	9.22
3-Methylbenzaldehyde	C_8H_8O	1.36
Benzoic acid	$C_7H_6O_2$	6.26
1-Ethyl-4-vinylbenzene	$C_{10}H_{12}$	1.52
2-Ethylphenol	$C_8H_{10}O$	2.26
2′-Hydroxyacetophenone	$C_8H_8O_2$	5.43
4-Ethylbenzaldehyde	$C_9H_{10}O$	2.24
4′-Ethylacetophenone	$C_{10}H_{12}O$	3.68
Biphenyl	$C_{12}H_{10}$	2.32
2,4-Di-tert-butylphenol	$C_{14}H_{22}O$	1.82
Dibenzofuran	$C_{12}H_8O$	2.28
Benzophenone	$C_{13}H_{10}O$	1.95
Xanthone	$C_{13}H_8O_2$	1.87
Anthraquinone	$C_{14}H_8O_2$	2.16

Table 7. Liquid-phase intermediates at 25 MPa, 460 °C, and initial COD of 60,000 mg·L^{-1}, identified at residence times of 1 min and 3.7 min.

Experiment with Residence Time of 1 min			Experiment with Residence Time of 3.7 min		
Compound	**Formula**	**Peak Area Ratio (%)**	**Compound**	**Formula**	**Peak Area Ratio (%)**
Phenol	C_6H_6O	4.42	4-Penten-1-ol	$C_5H_{10}O$	2.46
Benzoic acid	$C_7H_6O_2$	8.43	4,5-Dimethyl-2,6-octadiene	$C_{10}H_{18}$	7.82
4,5-Dimethyl-2,6-octadiene	$C_{10}H_{18}$	2.35	2,6-Dimethylnonane	$C_{11}H_{24}$	6.85
Phthalic anhydride	$C_8H_4O_3$	3.58	5-Methyltetradecane	$C_{15}H_{32}$	7.74
Phthalaldehydic Acid	$C_8H_6O_3$	4.62	Diethyl adipate	$C_{10}H_{18}O_4$	4.87
2-Hydroxymethylbenzoic acid	$C_8H_8O_3$	7.68	Methyl 10-oxohexadecanoate	$C_{17}H_{32}O_3$	2.34
Phthalic acid	$C_8H_6O_4$	8.71	trans-2,3-Epoxyoctane	$C_8H_{16}O$	1.85
2-Methyl-3-octanone	$C_9H_{18}O$	2.52	Tridecanoic acid	$C_{13}H_{26}O_2$	17.42
5-Methyl-Z-5-docosene	$C_{23}H_{46}$	3.74	Pentadecanoic acid	$C_{15}H_{30}O_2$	16.03
Tridecanoic acid	$C_{13}H_{26}O_2$	4.62			
Pentadecanoic acid	$C_{15}H_{30}O_2$	3.87			
Palmitic Acid	$C_{16}H_{32}O_2$	5.69			
(Z)-7-Hexadecenal	$C_{16}H_{30}O$	2.18			
Methyl 10-oxohexadecanoate	$C_{17}H_{32}O_3$	4.59			
Geranylgeranyl Alcohol	$C_{20}H_{34}O$	2.35			
Heneicosane	$C_{21}H_{44}$	3.46			

As shown in Table 6, the SCWO of cationic resin involves a complex series of reactions in the initial stage. The greatest variety of intermediates was detected at very short reaction times. The ion exchange resin is composed of polystyrene, which undergoes partial degradation under short reaction times. The intermediate products detected all contain benzene rings, including phenol, acetophenone, benzaldehyde, benzoic acid, 2′-hydroxyacetophenone, o-cymene, 4′-ethylacetophenone, and 2-methylphenol. Dimers such as dibenzofuran, benzophenone, and anthraquinone were also detected. The presence of a significant quantity of nitrogen-containing substances in anion resins during brief reaction times indicates that quaternary ammonium groups may participate in the subsequent degradation process of the resin skeleton [12,16,28]. The C–S bond linked to the sulfonic acid group in cationic resin requires less energy to break than the C–N and C–C bonds associated with the quaternary ammonium group in anionic resin, so sulfur-containing intermediates were absent and the sulfonic acid group dissociated first during the initial reaction stage [10].

As shown in Table 7, after 1 min, the intermediates consisted of aromatic compounds and aliphatic chain products. The aromatic compounds were mainly oxygenated aromatics, including phthalic acid, benzoic acid, 2-hydroxymethylbenzoic acid, benzaldehydic acid, phenol, and phthalic anhydride. The chain products were primarily oxygenated aliphatic organics such as palmitic acid, tridecanoic acid, and methyl 10-oxopalmitate,

together with non-oxygenated chain compounds, including 4,5-dimethyl-2,6-octadiene, 5-methyl-Z-5-docosene, and heneicosane. When the reaction time was extended to 3.7 min, the intermediates were similar to those observed in the degradation of anion exchange resins [12]. They were dominated by aliphatic compounds such as tridecanoic acid, pentadecanoic acid, and 5-methyltetradecane, with no aromatic compounds detected. This result indicates that the aromatic compounds gradually converted into open-chain products and were ultimately oxidized and removed.

As reported in our prior research [12], quaternary ammonium groups participate in the downstream degradation pathways of anion resin polymers. However, as shown in Tables 6 and 7, no sulfur-containing organic compounds were detected among the intermediates of cation exchange resin degradation, indicating that the sulfonic acid groups had dissociated from the polystyrene backbone at the initial stage of the reaction. Akai et al. [29] analyzed the liquid-phase products of waste cationic resins after supercritical water oxidation using ion chromatography, and confirmed that sulfonic acid groups were completely recovered in the form of SO_4^{2-}. Similar results have been reported by Kim et al. [7,11] and Lebroys et al. [10,16], with sulfur being identified as having been converted into sulfate during the SCWO of waste cation resins. Therefore, the transformation pathway of sulfonic acid groups in cation exchange resins is relatively straightforward: once dissociated from the polystyrene backbone, they are oxidized into sulfate and retained in the reaction system.

4.2. Mechanism Analysis

During the supercritical water oxidation process, the oxidation of organic compounds generally proceeds at very high reaction rates, sometimes even on the millisecond scale [30]. Therefore, detecting a wide variety of intermediates within any given reaction time is not straightforward. Based on the intermediates detected in this work, a simplified degradation pathway for waste cation exchange resins is tentatively proposed and illustrated in Figure 6.

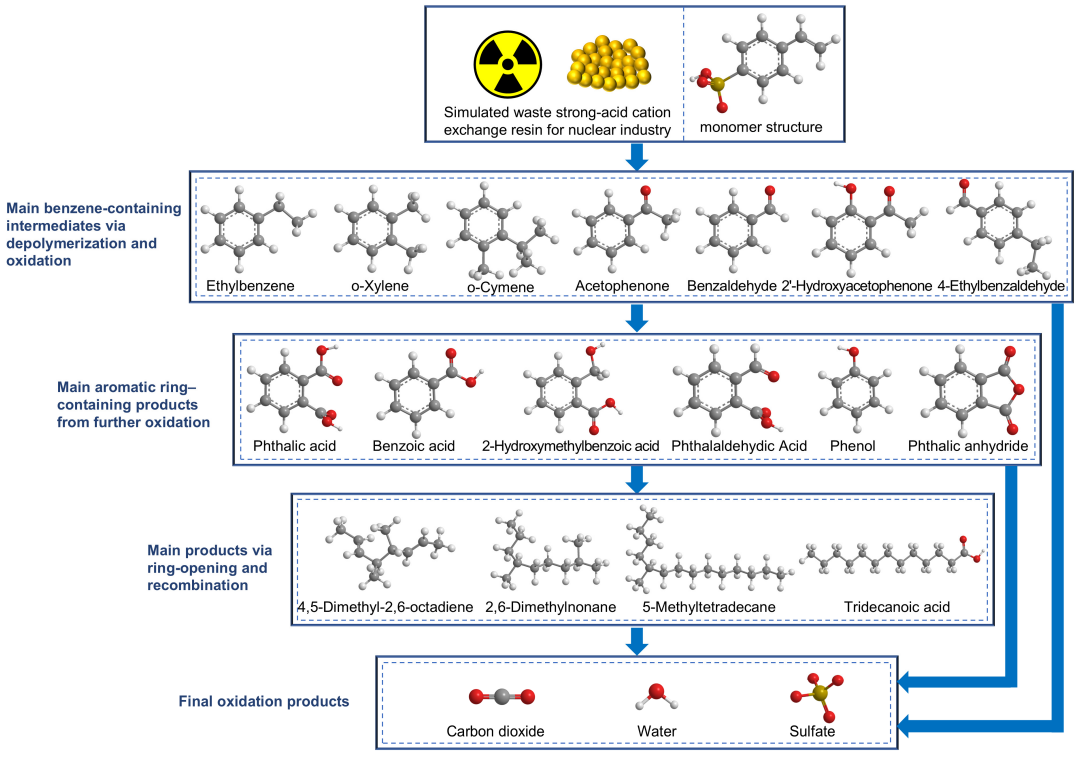


Figure 6. Simplified degradation pathway of cation exchange resins during SCWO proposed tentatively based on intermediates.

In this process, the polymers derived from strongly acidic cationic resins first underwent pyrolysis to form polymeric monomers [28,31,32], followed by complex reactions such as oxidation, ring opening, and recombination. Ultimately, they were transformed into small molecular substances, with aromatic compounds, particularly phenol, serving as important intermediates. Under extremely short reaction durations (Table 6), no sulfur-containing organic compounds were detected in the degradation intermediates. This suggests that the sulfonic acid group dissociated during the initial reaction stage and thus did not participate in subsequent reactions of the aromatic compounds. It should be noted that this pathway is based on the detected intermediates rather than on direct kinetic evidence.

For sulfur-containing organic compounds in supercritical water, degradation typically involves stepwise conversion to SO_4^{2-}. Based on previous studies and the intermediates detected in this study, the following steps are tentatively proposed for the transformation of sulfonic acid groups in cation exchange resins (Figure 6). Wang et al. [33] demonstrated that sulfur in coal can be progressively oxidized to sulfate via $S^{2-} \rightarrow S_2O_3^{2-} \rightarrow SO_3^{2-} \rightarrow SO_4^{2-}$ in low-temperature supercritical water (temperatures $\leq$ 420 °C), with enhanced conversion efficiency at elevated temperatures. In a model wastewater study using ammonium sulfide under supercritical water conditions (698.2–773.2 K, 22.0–30.0 MPa), S^{2-} was fully oxidized to SO_4^{2-} within less than 10 s [34]. For sulfonic acid groups in cation exchange resins, Aki et al. [29] reported their nearly complete conversion to sulfuric acid under SCWO conditions (673 K, 30 MPa, reaction time $\geq$ 3 min). Kim et al. [7,11] further confirmed that sulfonic acid functional groups in cation resins produce sulfuric acid during SCWO, while Dubōis et al. [35] observed complete transformation of all sulfonic groups into sulfate under supercritical water conditions (380 °C, 25.5 MPa). Additionally, benzenesulfonic acid and related compounds undergo desulfonation to form sulfuric acid when heated in water above 200 °C [36,37]. Thus, the decomposition of cation resins can be summarized in two main steps: removal of sulfonic groups from the benzene ring and oxidative cleavage of the polymer backbone. The overall oxidation reaction for cation resins can be represented as follows [7,11]:

$$4(C_{16}H_{15}O_3S)_n + 79nO_2 \rightarrow 64nCO_2 + 26nH_2O + 4nH_2SO_4 \quad \text{(R1)}$$

In the supercritical water environment, chemical reactions are generally dominated by free radical mechanisms [38]. The degradation of organic compounds is initiated by the abstraction of a hydrogen atom. In the presence of oxygen, organic compounds undergo oxidation to form R• and HO_2• (R2). Subsequently, HO_2• abstracts a hydrogen atom from the organic substrates, yielding R• and H_2O_2 (R3), while H_2O_2 further decomposes to produce OH• (R4), or directly undergoes thermal decomposition to form OH•. OH• is considered the predominant reactive species in SCWO, capable of reacting with a wide range of organic contaminants (R5) [39]. These radical reactions, consistent with the intermediates observed in this study, may lead to transformations of resin monomers, such as isomerization or alkyl transfer. These transformations result in the formation of ethylbenzene, o-xylene, and o-cymene [8,12]. The presence of biphenyl among the products suggested that an aromatic coupling reaction took place during the degradation of the organic compounds (Table 6).

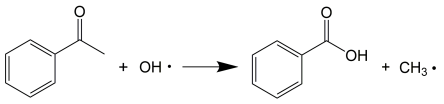
$$RH + O_2 \rightarrow R\bullet + HO_2\bullet \quad \text{(R2)}$$

$$RH + HO_2 \rightarrow R\bullet + H_2O_2 \quad \text{(R3)}$$

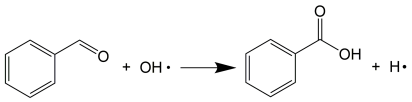
$$H_2O_2 \rightarrow 2OH\bullet \quad \text{(R4)}$$

$$RH + OH\bullet \rightarrow R\bullet + H_2O \quad (R5)$$

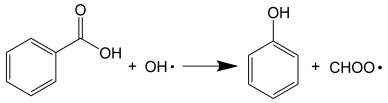
In supercritical water, aromatic compounds such as ethylbenzene, o-xylene, and o-cymene were progressively oxidized to oxygenated aromatic species, including acetophenone, benzaldehyde, 2′-hydroxyacetophenone, and 4-ethylbenzaldehyde. They were also converted into a series of aromatic acids, such as phthalic acid, benzoic acid, 2-hydroxymethylbenzoic acid, phthalaldehydic acid, and phthalic anhydride. These oxygenated aromatic intermediates were subsequently transformed into phenol via oxidation, decarboxylation, and hydroxylation reactions, involving the addition of OH• radicals to the α-carbon of the aromatic ring (R6–R8) [16].



(R6)



(R7)



(R8)

As a crucial intermediate, the conversion pathway of phenol under SCWO conditions generally follows the route proposed by Gopalan, S. and Savage, P.E. [40], as shown in Figure 7. The hydroxyl group of phenol influences the ring-opening reaction and can lead to the formation of several undesired polymerization products, including dibenzofuran, benzophenone, and xanthone [41,42]. Aromatic compounds subsequently undergo further oxidation accompanied by ring opening, generating low-molecular-weight carboxylic acids, such as acetic acid, and aliphatic hydrocarbon radicals. These small-molecule products can recombine, forming long-chain fatty acids and aliphatic hydrocarbons [35], which were detected in the liquid products and ultimately oxidized to CO_2 and H_2O [42].

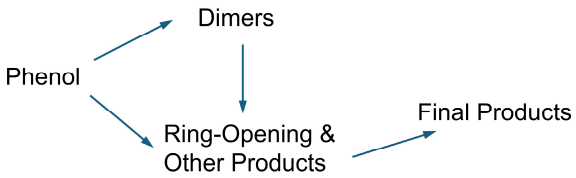


Figure 7. The oxidation reaction pathways of phenol in SCW [40].

In the SCWO of polystyrene resins functionalized with sulfonic acid groups, the addition of NaOH significantly enhanced the degradation efficiency, as shown in Figure 2. Although free radical reactions dominate in supercritical water, ionic reactions can still occur even at 773 K [43]. In supercritical water, NaOH undergoes incomplete ionization, existing partly as free reactive ions (OH^-, Na^+) and partly as ion-associated pairs [44]. In the presence of NaOH, the decomposition of organic compounds proceeds via both ionic and radical pathways [18], with OH^- and Na^+ ions synergistically promoting the reaction through multiple mechanisms.

First, OH^- from NaOH acts as a strong nucleophile, directly attacking carbon atoms in organic molecules and inducing bond cleavage. As reported by Lee et al. [18] and Liu et al. [45], OH^- can efficiently perform nucleophilic substitution under supercritical water conditions, replacing halogens or other electron-withdrawing groups. The sulfonic acid

group, being strongly electron-withdrawing [46], renders the attached aromatic carbon partially positive, creating an ideal site for nucleophilic attack. This nucleophilic substitution cleaves the C–S bond, effectively liberating the sulfonic group from the polymer backbone, thereby facilitating resin fragmentation and subsequent oxidation.

Second, Na^+ can interact with sulfonic acid-derived SO_4^{2-} intermediates (R1) to form ionic-dipole bonded species and ultimately Na_2SO_4, while the organic matter is degraded into final products. Additionally, during SCWO of organics, NaOH can react with acetic acid [16,47], a stable intermediate, as well as with final products such as CO_2, accelerating the overall reaction (R9–R11). Moreover, the resulting CH_3COONa is more readily oxidized than acetic acid itself [48]. Meanwhile, Na_2CO_3 formed in the products can act as a catalyst for ring-opening reactions of aromatic compounds [49].

$$CH_3COOH + NaOH \rightarrow CH_3COONa + H_2O \quad \text{(R9)}$$

$$2CH_3COONa + 4O_2 \rightarrow 3CO_2 + H_2O + Na_2CO_3 \quad \text{(R10)}$$

$$CO_2 + 2NaOH \rightarrow Na_2CO_3 + H_2O \quad \text{(R11)}$$

Furthermore, Lee et al. [18] reported that NaOH promotes the decomposition of phenolic intermediates and accelerates the formation of ring-opened products. Mansfield [50] showed that NaOH can specifically influence R–O_2• radical pathways. The alkaline environment provided by NaOH facilitates deprotonation of key intermediates (e.g., H_2O_2, HO_2•), generating more reactive anionic species (e.g., HO_2^-, O_2^-). This significantly increases the yield of oxygen-containing intermediates and guides the reaction along more efficient pathways, ultimately leading to a more complete reaction. These multiple effects demonstrate that NaOH plays a key promoting role in the SCWO of cation resins.

5. Conclusions

This study systematically investigated the degradation of strong acid cation exchange resins under SCWO conditions and optimized the process parameters using RSM. Controlled experiments evaluated the effects of reaction temperature, oxidant stoichiometry, initial organic concentration, and residence time. The established second-order polynomial model (with R^2 = 0.9951) accurately predicted R_{COD}, with experimental results closely matching model predictions. Among the tested variables, reaction temperature, oxidant stoichiometry, and residence time were identified as the most significant factors affecting degradation efficiency. A COD-dependent addition of 1.74 wt% NaOH under optimized conditions (472 °C, oxidant stoichiometry 137%, initial COD 77,216 mg·L^{-1}, and residence time 4.9 min) further enhanced resin decomposition, achieving an R_{COD} of 99.92%. Through analysis of degradation intermediates, the primary degradation pathway of typical resin intermediates was proposed: sulfonic groups dissociated early, followed by aromatic compounds, particularly phenol, undergoing ring-opening and oxidation to small carboxylic acids and aliphatic species, which were ultimately mineralized to CO_2 and H_2O.

These results provide mechanistic insight into resin degradation and establish a scientific basis for the safe and efficient treatment of radioactive waste resins using SCWO. While laboratory-scale experiments demonstrated clear trends in degradation and process optimization, further investigations on a pilot-scale SCWO system are necessary to confirm scalability and evaluate practical applicability. Future work will focus on the migration and solid-phase immobilization of radionuclides adsorbed on the resins, as well as potential corrosion issues arising from sulfate (SO_4^{2-}) produced during sulfonic group degradation and the addition of NaOH, with the aim of further optimizing SCWO applications and ensuring long-term safety and stability.

Author Contributions: Conceptualization, T.X. and Y.L.; resources, S.W. and D.X.; writing—original draft preparation, T.X. and Y.L.; writing—review and editing, T.X., Y.L., Q.Z., Y.J. and W.S.; All authors have read and agreed to the published version of the manuscript.

Funding: This research was funded by the National Natural Science Foundation of China (No. 22378322), the Shaanxi Province Key Research and Development Project of China (No. 2024GX-YBXM-424), the Doctoral Research Foundation of Xihang University (No. 2023KY0210/No. 2021KY0227/No. 2021KY0228).

Data Availability Statement: The original contributions presented in this study are included in this article. Further inquiries can be directed to the corresponding authors.

Conflicts of Interest: The authors declare no conflicts of interest.

References

1. Wang, J.; Wan, Z. Treatment and disposal of spent radioactive ion-exchange resins produced in the nuclear industry. *Prog. Nucl. Energy* **2015**, *78*, 47–55. [CrossRef]
2. Kritzer, P.; Dinjus, E. An assessment of supercritical water oxidation (SCWO)—Existing problems, possible solutions and new reactor concepts. *Chem. Eng. J.* **2001**, *83*, 207–214. [CrossRef]
3. Marrone, P.A. Supercritical water oxidation-Current status of full-scale commercial activity for waste destruction. *J. Supercrit. Fluids* **2013**, *79*, 283–288. [CrossRef]
4. Sugiyama, W.; Yamamura, T.; Park, K.C.; Tomiyasu, H.; Satoh, I.; Shiokawa, Y.; Okada, H.; Sugita, Y. Recovery of radioactivity as solids from nonflammable organic low-level radioactive wastes using supercritical water mixed with RuO_2. *J. Supercrit. Fluids* **2005**, *35*, 240–246. [CrossRef]
5. Wang, L.; Li, A.; Peng, Z.; Yi, L.; Chen, B.; Jin, H.; Chen, Y.; Guo, L. Investigation on the detailed mechanisms of cationic ion exchange resin gasification in supercritical water by ReaxFF reactive molecular dynamics simulation. *Biomass Bioenergy* **2025**, *193*, 107586. [CrossRef]
6. Wang, L.; Mao, L.; Li, A.; Peng, Z.; Yi, L.; Chen, B.; Jin, H.; Chen, Y.; Guo, L. Kinetic mechanism study of mixed ion exchange resins gasification in supercritical water. *Biomass Bioenergy* **2025**, *195*, 107708. [CrossRef]
7. Kim, K.; Son, S.H.; Kim, K.; Han, J.H.; Do Han, K.; Do, S.H. Treatment of radioactive ionic exchange resins by super- and sub-critical water oxidation (SCWO). *Nucl. Eng. Des.* **2010**, *240*, 3654–3659. [CrossRef]
8. Xu, T.T.; Wang, S.Z.; Li, Y.H.; Li, J.; Cai, J.; Zhang, Y.; Xu, D.; Zhang, J. Review of the destruction of organic radioactive wastes by supercritical water oxidation. *Sci. Total Environ.* **2021**, *799*, 149396. [CrossRef] [PubMed]
9. Sugiyama, W.; Park, K.C.; Yamamura, T.; Okada, H.; Sugita, Y.; Tomiyasu, H. Decomposition of radioactive organic wastes with supercritical water medium containing RuO_2. *J. Nucl. Sci. Technol.* **2005**, *42*, 256–258. [CrossRef]
10. Leybros, A.; Roubaud, A.; Guichardon, P.; Boutin, O. Ion exchange resins destruction in a stirred supercritical water oxidation reactor. *J. Supercrit. Fluids* **2010**, *51*, 369–375. [CrossRef]
11. Kim, K.; Kim, K.; Choi, M.; Son, S.H.; Han, J.H. Treatment of ion exchange resins used in nuclear power plants by super- and sub-critical water oxidation—A road to commercial plant from bench-scale facility. *Chem. Eng. J.* **2012**, *189–190*, 213–221. [CrossRef]
12. Xu, T.T.; Wang, S.Z.; Li, Y.H.; Zhang, J.; Li, J.; Zhang, Y.; Yang, C. Optimization and mechanism study on destruction of the simulated waste ion-exchange resin from the nuclear industry in supercritical water. *Ind. Eng. Chem. Res.* **2020**, *59*, 18269–18279. [CrossRef]
13. Tang, X.; Zheng, Y.; Liao, Z.; Wang, Y.; Yang, J.; Cai, J. A review of developments in process flow for supercritical water oxidation. *Chem. Eng. Commun.* **2021**, *208*, 1494–1510. [CrossRef]
14. Yu, G.; Hu, D. Simulation and optimization of supercritical water oxidation processes. *Desalination Water Treat.* **2023**, *295*, 191–204.
15. Sadri Moghaddam, S.; Alavi Moghaddam, M.R.; Arami, M. Coagulation/flocculation process for dye removal using sludge from water treatment plant: Optimization through response surface methodology. *J. Hazard. Mater.* **2010**, *175*, 651–657. [CrossRef]
16. Leybros, A.; Roubaud, A.; Guichardon, P.; Boutin, O. Supercritical water oxidation of ion exchange resins: Degradation mechanisms. *Process Saf. Environ. Prot.* **2010**, *88*, 213–222. [CrossRef]
17. Kritzer, P. Corrosion in high-temperature and supercritical water and aqueous solutions: A review. *J. Supercrit. Fluids* **2004**, *29*, 1–29. [CrossRef]
18. Lee, G.; Nunoura, T.; Matsumura, Y.; Yamamoto, K. Comparison of the effects of the addition of NaOH on the decomposition of 2-chlorophenol and phenol in supercritical water and under supercritical water oxidation conditions. *J. Supercrit. Fluids* **2002**, *24*, 239–250. [CrossRef]
19. Feng, X.; Liu, Y.; Li, X.; Liu, H. RSM, ANN-GA and ANN-PSO modeling of SDBS removal from greywater in rural areas via Fe_2O_3-coated volcanic rocks. *RSC Adv.* **2022**, *12*, 6265–6278. [CrossRef]

20. Zewide, Y.T.; Yemata, T.A.; Ayalew, A.A.; Kedir, H.J.; Tadesse, A.A.; Fekad, A.Y.; Shibesh, A.K.; Getie, F.A.; Tessema, T.D.; Wubieneh, T.A.; et al. Application of response surface methodology (RSM) for experimental optimization in biogenic silica extraction from rice husk and straw ash. *Sci. Rep.* **2025**, *15*, 132. [CrossRef] [PubMed]
21. Thornton, T.D.; Savage, P.E. Kinetics of phenol oxidation in supercritical water. *AIChE J.* **1992**, *38*, 321–327. [CrossRef]
22. Savage, P.E. Organic Chemical Reactions in Supercritical Water. *Chem. Rev.* **1999**, *99*, 603–622. [CrossRef]
23. Vogel, F.; Blanchard, J.L.D.; Marrone, P.A.; Rice, S.F.; Webley, P.A.; Peters, W.A.; Smith, K.A.; Tester, J.W. Critical review of kinetic data for the oxidation of methanol in supercritical water. *J. Supercrit. Fluids* **2005**, *34*, 249–286. [CrossRef]
24. Ma, H.; Shen, M.; Tong, Y.; Wang, X. Radioactive Wastewater Treatment Technologies: A Review. *Molecules* **2023**, *28*, 1935. [CrossRef] [PubMed]
25. Vera Candioti, L.; De Zan, M.; Cámara, M.; Goicoechea, H. Experimental design and multiple response optimization. Using the desirability function in analytical methods development. *Talanta* **2014**, *124*, 123–138. [CrossRef] [PubMed]
26. Myers, R.H.; Montgomery, D.C.; Anderson-Cook, C. *Response Surface Methodology: Process and Product Optimization Using Designed Experiments*, 4th ed.; Wiley: Hoboken, NJ, USA, 2016.
27. Körbahti, B.K.; Aktaş, N.; Tanyolaç, A. Optimization of electrochemical treatment of industrial paint wastewater with response surface methodology. *J. Hazard. Mater.* **2007**, *148*, 83–90. [CrossRef]
28. Wang, L.; Yi, L.; Wang, G.; Li, L.; Lu, L.; Guo, L. Experimental investigation on gasification of cationic ion exchange resin used in nuclear power plants by supercritical water. *J. Hazard. Mater.* **2021**, *419*, 126437. [CrossRef]
29. Akai, Y.; Yamada, K.; Sako, T. Ion-exchange resin decomposition in supercritical water. *High Press. Res.* **2001**, *20*, 515–524. [CrossRef]
30. Onwudili, J.A.; Williams, P.T. Flameless incineration of pyrene under sub-critical and supercritical water conditions. *Fuel* **2006**, *85*, 75–83. [CrossRef]
31. Liu, Z.; Chen, M.; Li, B. Experimental evaluation on pyrolysis and gasification characteristics of simulated waste cation exchange resin. *J. Therm. Anal. Calorim.* **2024**, *149*, 10965–10982. [CrossRef]
32. Luo, J.; Zhou, X.; Tong, W.; Du, X.; Li, P.; Zhang, Y. Oxidative pyrolysis of ion exchange resin in the presence of manganese dioxide: Product analysis, conversion and simplification mechanism. *J. Environ. Chem. Eng.* **2023**, *11*, 110695. [CrossRef]
33. Wang, T.; Zhu, X. Sulfur transformations during supercritical water oxidation of a Chinese coal. *Fuel* **2003**, *82*, 2267–2272. [CrossRef]
34. Wang, T.; Xiang, B.; Liu, J.; Shen, Z. Supercritical Water Oxidation of Sulfide. *Environ. Sci. Technol.* **2003**, *37*, 1955–1961. [CrossRef] [PubMed]
35. Dubois, M.A.; Dozol, J.F.; Massiani, C.; Ambrosio, M. Reactivities of polystyrenic polymers with supercritical water under nitrogen or air. Identification and formation of degradation compounds. *Ind. Eng. Chem. Res.* **1996**, *35*, 2743–2747. [CrossRef]
36. Scholz, D.; Kröcher, O.; Vogel, F. Deactivation and Regeneration of Sulfonated Carbon Catalysts in Hydrothermal Reaction Environments. *ChemSusChem* **2018**, *11*, 2189–2201. [CrossRef]
37. Geethanjali, R.; Subhashini, S. Functionalization of PVA to synthesize p-vinyl benzene sulfonate terpolymers—A comparative study of anticorrosion, adsorption and activation properties of the terpolymers on mild steel in 1 M HCl. *RSC Adv.* **2016**, *6*, 100748–100758. [CrossRef]
38. Xu, T.T.; Wang, S.Z.; Tang, X.Y.; Li, Y.; Yang, J.; Li, J.; Zhang, Y. Corrosion mechanism of inconel 600 in oxidizing supercritical aqueous systems containing multiple salts. *Ind. Eng. Chem. Res.* **2019**, *58*, 23046–23056. [CrossRef]
39. Li, L.X.; Chen, P.S.; Gloyna, E.F. Generalized kinetic-model for wet oxidation of organic-compounds. *AIChE J.* **1991**, *37*, 1687–1697. [CrossRef]
40. Gopalan, S.; Savage, P.E. A reaction network model for phenol oxidation in supercritical water. *AIChE J.* **1995**, *41*, 1864–1873. [CrossRef]
41. Onwudili, J.A.; Williams, P.T. Reaction mechanisms for the decomposition of phenanthrene and naphthalene under hydrothermal conditions. *J. Supercrit. Fluids* **2007**, *39*, 399–408. [CrossRef]
42. Gopalan, S.; Savage, P.E. Reaction mechanism for phenol oxidation in supercritical water. *J. Phys. Chem.* **1994**, *98*, 12646–12652. [CrossRef]
43. Savage, P.E.; Gopalan, S.; Mizan, T.I.; Martino, C.J.; Brock, E.E. Reactions at supercritical conditions: Applications and fundamentals. *AIChE J.* **1995**, *41*, 1723–1778. [CrossRef]
44. Ma, J.; Dong, X.; Yu, Y.; Zheng, B.; Zhang, M. The effects of alkalis on the dechlorination of o-chlorophenol in supercritical water: Molecular dynamics simulation and experiment. *Chem. Eng. J.* **2014**, *241*, 268–272. [CrossRef]
45. Liu, K.; Zhang, Z.; Zhang, F.-S. Advanced degradation of brominated epoxy resin and simultaneous transformation of glass fiber from waste printed circuit boards by improved supercritical water oxidation processes. *Waste Manag.* **2016**, *56*, 423–430. [CrossRef] [PubMed]
46. Domingo, L.R.; Ríos-Gutiérrez, M.; Aurell, M.J. Unveiling the regioselectivity in electrophilic aromatic substitution reactions of deactivated benzenes through molecular electron density theory. *New J. Chem.* **2021**, *45*, 13626–13638. [CrossRef]

47. Cui, B.-c.; Liu, S.-z.; Cui, F.-y.; Jing, G.-l.; Liu, X.-j. Lumped kinetics for supercritical water oxidation of oily sludge. *Process Saf. Environ. Prot.* **2011**, *89*, 198–203. [CrossRef]
48. Takahashi, F.; Oshima, Y.; Fukushi, K.; Yamamoto, K. Enhanced Oxidation of Alkali Metal Acetate in Supercritical Water. *Chem. Lett.* **2012**, *41*, 267–269. [CrossRef]
49. Muthukumaran, P.; Gupta, R.B. Sodium-Carbonate-Assisted Supercritical Water Oxidation of Chlorinated Waste. *Ind. Eng. Chem. Res.* **2000**, *39*, 4555–4563. [CrossRef]
50. Mansfield, A. Experimental and Modeling Study of the Effects of NaOH on Propane Oxidation Kinetics in Supercritical Water. *Ind. Eng. Chem. Res.* **2025**, *64*, 13060–13066. [CrossRef]

Disclaimer/Publisher's Note: The statements, opinions and data contained in all publications are solely those of the individual author(s) and contributor(s) and not of MDPI and/or the editor(s). MDPI and/or the editor(s) disclaim responsibility for any injury to people or property resulting from any ideas, methods, instructions or products referred to in the content.